Analyzing the Effect of Monochromatic Aberrations on The Performance of a Cassegrain Telescope

Mohamed Ali[1], Mohamed Abdo M[2], Hany M. Mohamed[1], Mohamed A Ali[3], and Mohamed E Hanafy[3]

[1]Aircraft Armament Department, Military Technical College, Cairo, Egypt.
[2]Engineering Physics Department, Military Technical College, Cairo, Egypt.
[3]Aircraft Electrical Equipment Department, Military Technical College, Cairo, Egypt.

E-mail: mohamedali3296@gmail.com

Abstract. Monochromatic aberrations due to various optical elements of Cassegrain telescopes cause distortions and imperfections in acquired images. Hence, degrading their spatial resolution and overall quality. In this paper, the effects of three types of monochromatic aberrations, including coma, and astigmatism, spherical aberrations, of a Cassegrain telescope are comprehensively characterized. Zernike polynomials are employed to express and simulate these aberrations and to systematically analyse their impact on image quality. Quantitative metrics such as Mean Square Error (MSE), Peak-Signal to Noise Ratio (PSNR), and structural similarity index (SSIM) are utilized to assess the deviations introduced by aberrations compared to a diffraction-limited optical system. By applying these aberrations to spoke target image, this research contributes valuable insights into the specific context of Cassegrain telescopes. The findings provide a foundational understanding of aberration effects on high-resolution images to compromise an enhanced optical design.

1. Introduction

Aberrations in the wavefront of light propagating through an optical system, that contains refractive and reflective elements, directly affect image quality [1]. Sources of aberration vary according to different factors. Lens aberrations can originate from the optical design and manufacturing process of the imaging system. Imperfections in the lens elements include surface irregularities and non-uniformities in the glass. Coma aberration causes off-axis light rays to focus at different distances from the lens, resulting in distorted and comet-shaped images of point sources [2]. Astigmatism aberration is another significant optical phenomenon that affects the performance of lenses. This aberration occurs when light rays, passing through different meridians of a lens, have different focal points distorting the shape of images. In the context of astigmatism, point sources can appear elongated or stretched in one direction, leading to a degradation in image quality. Spherical aberration occurs when light rays passing through different parts of a lens converge at different focal points. This can lead to blurring and a loss of image resolution. On the other hand, reflective optical systems, such as conventional Cassegrain systems, consist of two curved mirrors known as primary and secondary mirrors. These systems are frequently employed in focusing and imaging applications, offering the benefits of a reduced system length when compared to single-lens systems. The optical functionality of these reflective systems depends on the accurate surface profiles of the curved mirrors, highlighting the importance of precise mirror shaping to achieve desired optical outcomes [3]. The Modulation Transfer Function (MTF) is usually used to describe the quality of an optical system. The ideal MTF for an optical system would have a value of unity for all spatial frequencies. In other words, it would transmit all spatial frequencies with perfect contrast and no degradation. However, this is unattainable in practical optical systems due to various physical limitations, including the fundamental effects of diffraction [1]. Zernike polynomials, which form a complete orthogonal basis set, are well-suited by Vasudevan L. and Andre Fleck for describing wavefronts of optical systems with circular pupils. This paper provides a brief overview of Zernike polynomial properties used to express and analyze different types of monochromatic aberrations [4, 5]. Weili Li et al carried out a study to outline an improvement in single-lens imaging by adding lenses to correct chromatic aberrations. It simplifies the point spread function (PSF) estimation through a blind image deconvolution method and enhances accuracy with Gaussian regularization, resulting in high-quality image restoration [6]. Yixing Ding et al illustrated that aberration deviation is attributed to reduced light time effects [7]. Francisco Avila discusses the development of a novel blind-deconvolution-based algorithm to correct spherical aberration and scattering effects. The approach, founded on theoretical functions derived from aberration theory and classical Zernike theory, significantly enhances image sharpness by 170% without prior knowledge of the optical system's PSF [8]. In this paper, the effects of coma, astigmatism and spherical aberrations of a Cassegrain telescope are expressed using Zernike polynomials. The MTFs of an optical system affected by these aberrations are investigated and applied upon a spoke target. Quantitative metrics including MSE, PSNR, and SSIM are then utilized to assess the deviations introduced by aberrations compared to a diffraction-limited optical system.

This paper is organized as follows: the second section overviews Zernike polynomial and its mathematical model. In the third section, the configuration of a classical Cassegrain telescope is described. The effect of various types of monochromatic aberrations on the performance of Cassegrain telescopes is investigated in the fourth section. Conclusions are given in the fifth section.

2. Zernike Polynomials

Two-dimensional Zernike polynomials serve as a powerful mathematical framework for characterizing the distortions present in the wavefront within the circular aperture of an optical system [9]. When expressed in polar coordinates (ρ, θ), where ρ is radial distance and θ is the azimuthal angle, these polynomials provide a comprehensive representation of the wavefront aberrations across the entire circular pupil of the optical system, as shown in figure 1 [8]. In essence, this expansion entails a series of orthonormal polynomials, known as Zernike polynomials, which elegantly encapsulate the intricate distortions and irregularities that can occur within the entrance aperture of an optical system. Such a precise description of wavefront aberrations is indispensable for various applications in optics, including wavefront correction, adaptive optics, and aberration analysis contributing to the refinement of optical systems and the enhancement of their performance. Zernike polynomials can be expressed by [9]:

$$W(\rho,\theta) = \sum_{n,m} C_n^m \, Z_n^m \, (\rho,\theta) \qquad (1)$$

Where, W represents the wavefront function, n, and m are nonnegative integers which specify the order and orientation of the inherent aberrations with n ≥ m ≥ 0, C_n^m are Zernike coefficients or amplitudes, and Z_n^m are Zernike polynomials.

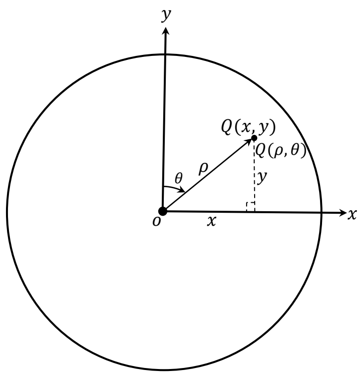

Figure 1. Cartesian (x,y) and polar (ρ,θ) coordinates of a point Q in the plane of a unit circle representing a circular exit pupil of an imaging system [8].

The Zernike polynomials, when presented in polar coordinates with x = ρ sin θ and y = ρ cos θ, are mathematically defined as a complex combination as follows [9]:

$$Z_n^m(\rho,\theta) \pm Z_n^{-m}(\rho,\theta) = V_n^{-m}(\rho\, cos\theta, \rho\, sin\theta) \quad (2)$$

$$Z_n^m(\rho,\theta) \pm Z_n^{-m}(\rho,\theta) = R_n^m(\rho)\exp(\pm im\theta) \quad (3)$$

Where V represents the radial polynomial associated with the Zernike polynomial, and R represents the angular polynomial associated with the Zernike polynomial. Then equations 2, and 3 can mathematically be represented as follows:

$$Z_n^m(\rho,\theta) = R_n^m(\rho)\cos(m\theta) \quad for\ m \geq 0 \quad (4)$$
$$Z_n^{-m}(\rho,\theta) = R_n^m(\rho)\cos(m\theta) \quad for\ m < 0 \quad (5)$$

The values of m and n, given in equations (1-5), determine the type of monochromatic aberrations. Each of these Zernike polynomials represents a distinct aberration type of a specific order n and orientation m, and the coefficient of the polynomial determines the magnitude and orientation of aberration in a given optical system. For coma aberration, the possible combinations of m values are ±1, and n values are 3, 5, and 7. For astigmatism aberration, the values of m are typically ±2, and n values are 2, 4, and 6 representing astigmatism along two orthogonal meridians (usually at 45 degrees apart). Spherical aberration is a specific type of aberration that causes all rays parallel to the optical axis to converge or diverge at different points, leading to a defocused image. Although the layout of the mirrors of a classical Cassegrain telescope eliminates the effect of lower order spherical aberrationas, higher order spherical aberrations still present [13]. Unlike other aberrations like coma or astigmatism, spherical aberration does not have an azimuthal variation, so m remains zero for all orders [9]. Table 1 lists the values of n and m for Zernike polynomials representing coma, astigmatism, and spherical aberrations.

Table 1. Types of Spherical, Coma, and Astigmatism Aberrations Using Zernike Orders/Orientations [9].

Aberration type	Order (n)	Orientation (m)
Coma	3/5/7	± 1
Astigmatism	2/4/6	± 2
Spherical	4/6/8	0

3. Classical Cassigrain Telescope Configuration

The classical Cassegrain telescope is a reflecting telescope that incorporates a specific optical configuration, providing a design that effectively addresses some of the challenges associated with traditional telescopes. In this configuration, which is shown in figure 2, light enters the telescope through a parabolic primary mirror, which reflects the incoming light to a smaller hyperbolic secondary mirror. The secondary mirror then reflects the light through a hole in the primary mirror, creating the final image. This design results in a folded optical path, allowing for a more compact telescope tube compared to a Newtonian telescope of equivalent focal length.

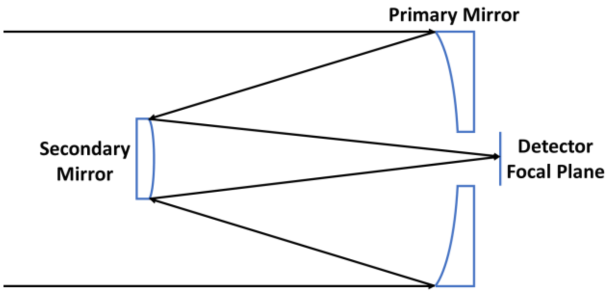

Figure 2. Cassegrain telescope configuration [10].

One advantage of the classical Cassegrain design is its compact and portable nature, making it suitable for both amateur astronomers and professional observatories. The folded optical path reduces the overall length of the telescope, making it easier to transport and store. Additionally, this design minimizes the effects of tube currents, enhancing image stability and reducing image distortion. The Cassegrain configuration also allows for the incorporation of various instruments, such as cameras and spectrometers, at the prime focus or secondary focus, adding versatility to its applications [10]. However, there are some disadvantages to the classical Cassegrain design. One notable drawback is the presence of a central obstruction caused by the secondary mirror, which can reduce the overall contrast and resolution of the telescope. This effect is particularly relevant for planetary observations and high-contrast imaging. Additionally, the optical elements of the Cassegrain system may introduce optical aberrations, although advanced designs and careful manufacturing can mitigate these issues to a certain

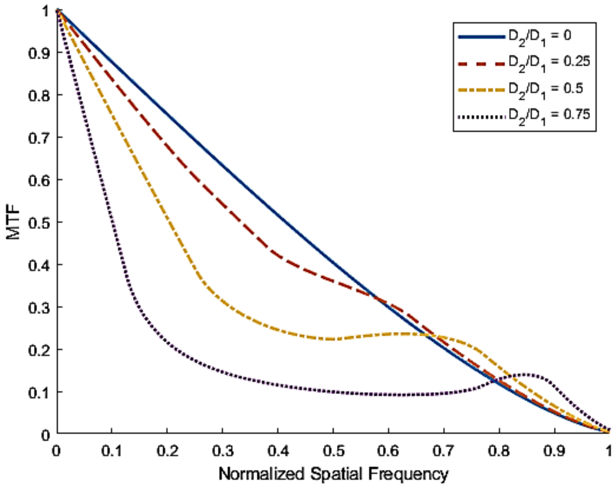

Figure 3. MTF for a Diffraction-limited Cassegrain Telescope with Various Obscuration Ratios [10].

extent [11]. In summary,
the classical Cassegrain telescope offers a compact and versatile design with advantages such as portability and reduced tube currents. However, it comes with trade-offs, including a central obstruction and potential optical aberrations that may impact image quality, particularly in specific observational scenarios.
Figure 3 shows MTF plots for a diffraction-limited Cassegrain telescope with various obscuration ratios (D_2/D_1), where D_1 is the diameter of the primary mirror and D_2 is the diameter of the secondary mirror.

4. Effect Of Monochromatic Aberrations On The Performance Of A Cassegrain Telescope

The experimental work of simulating the aberrations effect in degrading the quality of images acquired by a Cassegrain telescope can be investigated through the following steps:

Step 1: Construct the MTF curve of a diffraction-limited Cassegrain telescope, assuming an obscuration ratio of 0.25.

Step 2: Simulating the MTFs corresponding to various types of monochromatic aberrations, including coma, astigmatism, and spherical aberrations. These MTFs are simulated using Zernike polynomials and according to values of m and n given in Table. I.

Step 3: Applying MTFs of the diffraction-limited Cassegrain telescope and monochromatic aberrations on a spoke target.

Step 4: Using quality metrics, including PSNR, MSE, and SSIM to assess the degrading effect due to different aberration types. Figures (4- 6) show the MTF curves corresponding to coma, astigmatism, and spherical aberrations with different orders, respectively. Each order of aberration has a distinct MTF curve, where each aberrated MTF decreases the quality of the acquired image compared to the quality of an image produced by a diffraction-limited system.

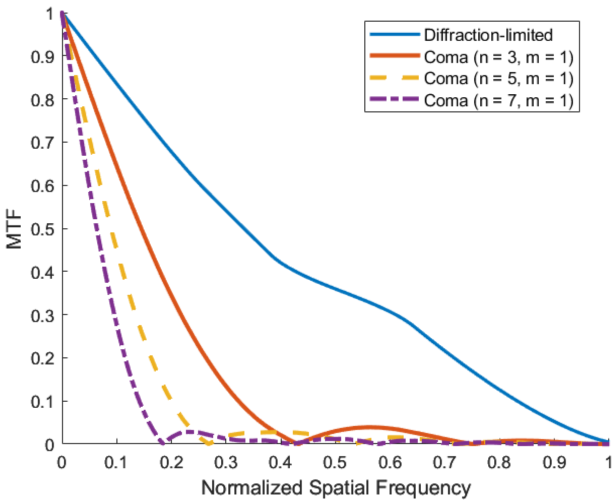

Figure 4. MTF Curves for Diffraction-limited System and Coma with Different Orders.

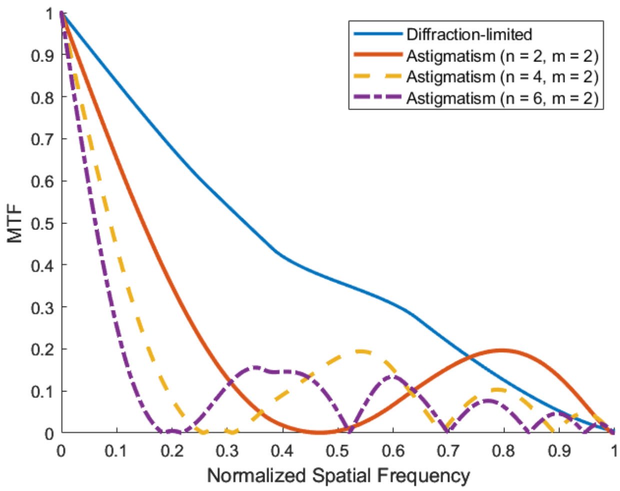

Figure 5. MTF Curves for Diffraction-limited System and Astigmatism with Different Orders.

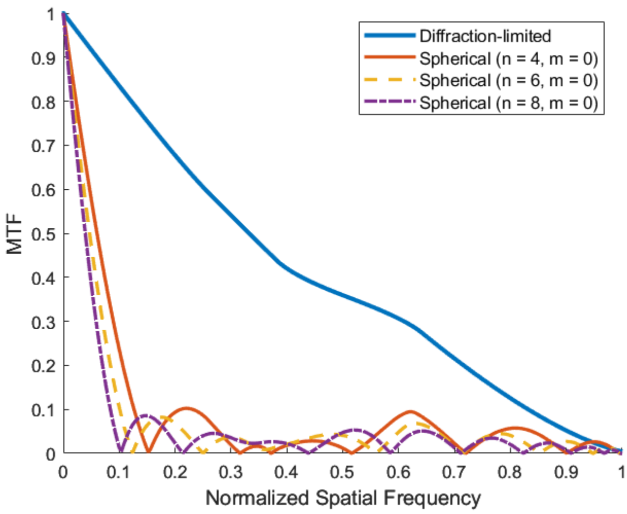

Figure 6. MTF Curves for a Diffraction-limited System and Spherical Aberration with Different Orders.

The resulting MTFs due to different orders of coma, astigmatism, and spherical aberrations are then applied to the spoke target given in figure 7. The aberrated images corresponding to the aberrated MTFs given in Figures (4-6) are shown in figure 8.

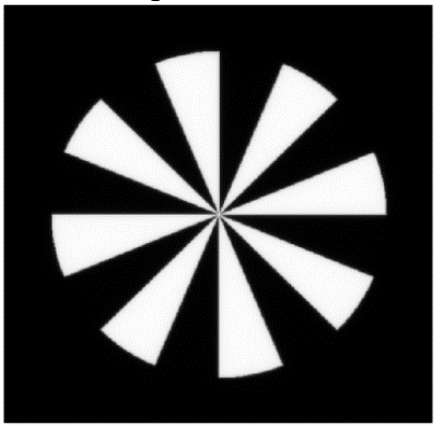

Figure 7. Spoke target.

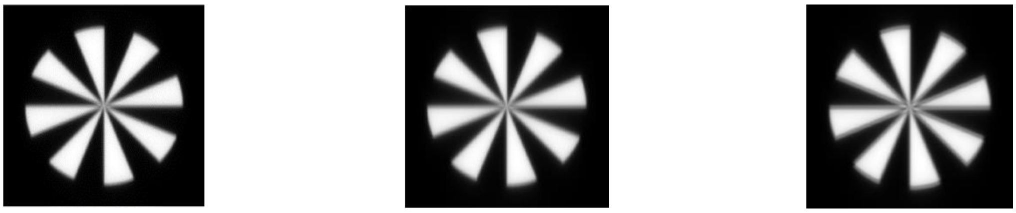

n= 3, m= 1 | n= 4, m= 1 | n= 5, m= 1

(a) Coma, with n = 3, 4, 5, and m = 1.

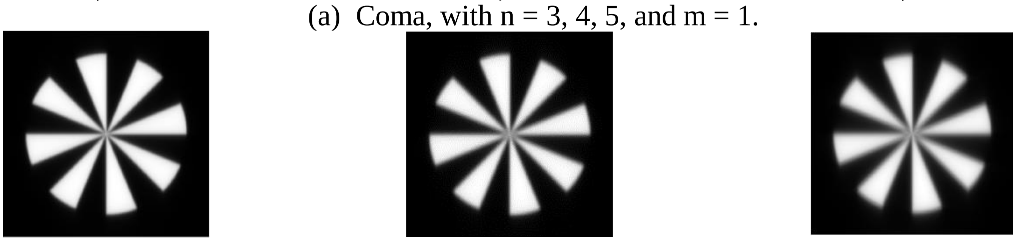

n= 3, m= 2 | n= 4, m= 2 | n= 5, m= 2

(b) Astigmatism, with n = 3, 4, 5, and m = 2.

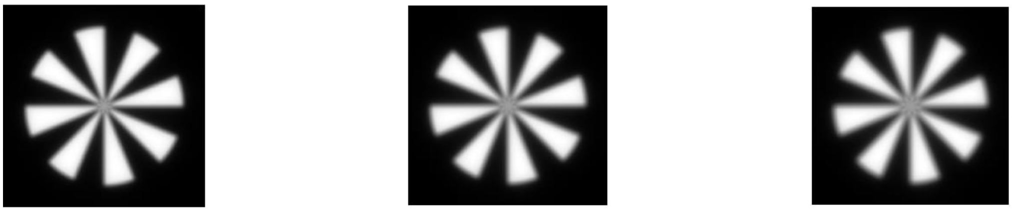

n= 4, m= 0 | n= 6, m= 0 | n= 8, m= 0

(c) Spherical Aberrations, with n = 4, 6, 8, and m = 0.

Figure 8. Degraded images due to different types of aberrations.

To quantitatively assess the extent of degradation caused by aberrations introduced by Zernike polynomials, we rely on PSNR, MSE, and SSIM. These metrics provide valuable insights about the degradation in image quality, enabling a more precise evaluation of the impact of aberrations, regardless of their order. The mathematical expression and more details about each metric can be found in [12].
Table 2 illustrates the assessment of degradation in image quality due to monochromatic aberrations using image quality metrics including PSNR, MSE, and SSIM. The values obtained valuable insights into the extent and nature of image degradation caused by these aberrations. All aberration types exhibit a similar trend of decreasing PSNR with increasing aberration severity. The MSE values consistently increase with worsening aberrations. SSIM values decrease across all aberration types,

indicating a decline in structural similarity upon increased aberration order. Spherical aberration tends to have the greatest impact on image quality.

It consistently shows the lowest PSNR, highest MSE, and lowest SSIM among the tested aberrations. Figures (9-11) illustrate the results for each type of aberration in a bar plot to facilitate comparing the assessments given in Table 2.

Table 2. Assessment of degradation in image quality using PSNR, MSE, and SSIM.

Aberration type	**(n, m)**	**PSNR**	**MSE**	**SSIM**
Coma	(3, 1)	21.21	0.0075	0.7058
	(5, 1)	18.18	0.0152	0.5699
	(7, 1)	16.21	0.0239	0.4682
Astigmatism	(2, 2)	23.80	0.0041	0.7970
	(4, 2)	20.35	0.0092	0.6687
	(6, 2)	18.12	0.0154	0.5649
Spherical Aberration	(4, 0)	18.63	0.0137	0.5515
	(6, 0)	17.27	0.0187	0.4759
	(8, 0)	16.29	0.0235	0.4243

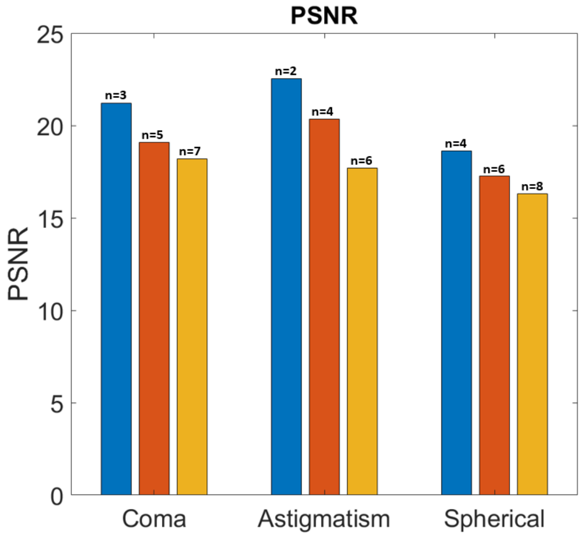

Figure 9. PSNR results of each type of aberration.

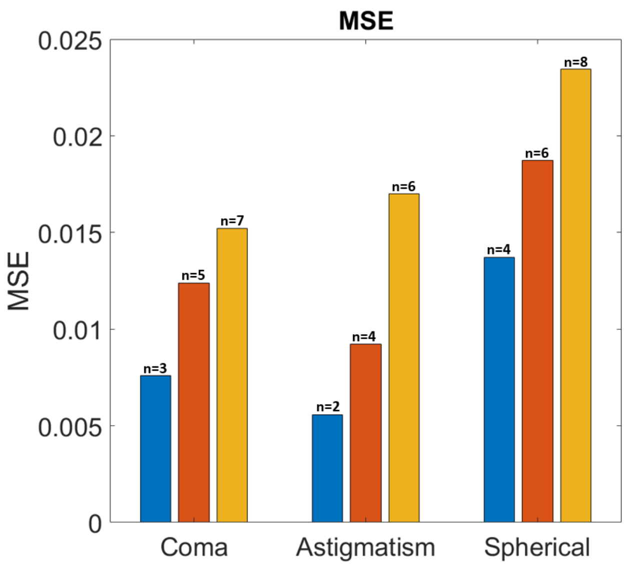

Figure 10. MSE results of each type of aberration.

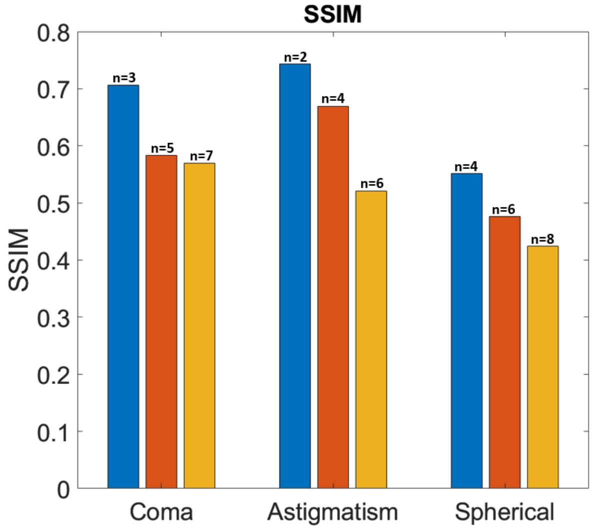

Figure 11. SSIM results of each type of aberration.

The obtained results align with the common understanding of spherical aberration as a significant aberration that can result in blurring and reduced image quality, which is reflected in the lower PSNR and higher MSE values. Also, as the order of aberration gets higher the chances of getting poor-quality images get higher.

5. Conclusions

In this study, we conducted a thorough examination of optical aberrations, specifically within the context of a Cassegrain telescope. Recognizing the inherent challenges posed by the telescope's optical design, including the presence of an obscuration, our investigation incorporated these factors into the evaluation of various aberration types. Utilizing Zernike polynomials, we systematically simulated and analyzed aberrations such as coma, astigmatism, and spherical aberration. The consideration of the telescope's design intricacies, including the obscuration, adds a layer of realism to our findings and enhances the applicability of our results to applied telescope configurations.
Zernike polynomials are effective quantitative tools that address the impact of monochromatic aberrations on image quality. Our approach, which integrates theoretical knowledge, simulation methodologies, and a telescope-specific context, contributes not only to a deeper understanding of aberration effects but also to the broader field of optical design. By addressing the complexities introduced by the Cassegrain telescope.
Through the construction of MTF curves and the application of quality metrics like PSNR, MSE, and SSIM, we gained precise insights into the extent of image degradation under different aberration scenarios. Spherical aberration emerged as a particularly influential factor, consistently exhibiting the most significant impact on image quality among the tested aberrations.

REFERENCES

[1] Carlsson, Kjell. "Imaging physics." KTH Applied Physics, Stockholm 2009.
[2] J. F. James, “Optical aberrations,” in Cambridge University Press eBooks, 2007, pp. 28–40. doi: 10.1017/cbo9780511534799.005.
[3] S. Yue et al., “Design and numerical analysis of an infrared Cassegrain telescope based on reflective metasurfaces,” Nanomaterials, vol. 11, no. 11, p. 2904, Oct. 2021, doi: 10.3390/nano11112904.
[4] V. Lakshminarayanan and A. Fleck, “Zernike polynomials: a guide,” Journal of Modern Optics, vol. 58, no. 7, pp. 545–561, Apr. 2011, doi: 10.1080/09500340.2011.554896.

[5] A. J. Del Águila-Carrasco, S. A. Read, R. Montés-Micó, and D. R. Iskander, “The effect of aberrations on objectively assessed image quality and depth of focus,” Journal of Vision, vol. 17, no. 2, p. 2, Mar. 2017, doi: 10.1167/17.2.2.
[6] W. Li, X.-C. Yin, Y. Liu, and M. Zhang, “Computational imaging through chromatic aberration corrected simple lenses,” Journal of Modern Optics, vol. 64, no. 20, pp. 2211–2220, Jul. 2017, doi: 10.1080/09500340.2017.1347723.
[7] Y. Ding, H. Guo, J. Dong, G. Liu, C. Han, and Z. Ruan, “Aberration effects in orbital imaging,” Remote Sensing Letters, vol. 10, no. 8, pp. 816–825, May 2019, doi: 10.1080/2150704x.2019.1612116.
[8] F. J. Ávila, “Spherical aberration and scattering compensation in digital imaging by a new blind deconvolution method,” Research Square (Research Square), May 2022, doi: 10.21203/rs.3.rs-1585245/v1.
[9] K. Niu and C. Tian, “Zernike polynomials and their applications,” Journal of Optics, vol. 24, no. 12, p. 123001, Nov. 2022, doi: 10.1088/2040-8986/ac9e08.
[10] M. F. Ali, A. S. Mohamed, H. M. Mohamed, and M. E. Hanafy, “Modeling and Analysis of a Cassegrain Telescope for Infrared Applications,” 2023 5th Novel Intelligent and Leading Emerging Sciences Conference (NILES), Oct. 2023, doi: 10.1109/niles59815.2023.10296800.
[11] A. Romano, Geometric Optics: Theory and design of astronomical optical systems using Mathematica®. 2010. [Online]. Available: http://ci.nii.ac.jp/ncid/BB00508800
[12] D. R. I. M. Setiadi, “PSNR vs SSIM: imperceptibility quality assessment for image steganography,” Multimedia Tools and Applications, vol. 80, no. 6, pp. 8423–8444, Nov. 2020, doi: 10.1007/s11042-020-10035-z.
[13] Sacek, Vladimir. “Notes on amateur telescope optics, 2006.” Journal of the Antique Telescope Society ”, vol. 28, no. 1, 2006, pp. 6-9.